GEOPHYSICAL RESEARCH LETTERS, VOL. 25, NO. 8, PAGES 1161-1164, APRIL 15, 1998

On the radiative properties of contrail cirrus

K. N. Liou[1], P. Yang[1], Y. Takano[1], K. Sassen[2], T. Charlock[3], and W. Arnott[4]

Abstract. Using the observed ice crystal size distribution in contrail cirrus from SUCCESS, we have carried out the scattering and absorption calculations based on a unified theory for light scattering by ice crystals covering all sizes and shapes. We illustrate the effects of ice crystal size and surface roughness on the scattering phase function features for remote sensing applications. The extinction coefficient and single-scattering albedo exhibit a minimum feature at 2.85 μm, referred to as the Christiansen effect, which is particularly pronounced for clouds consisting of a significant number of small ice crystals. Based on a line-by-line equivalent solar model, we show from spectral curves that cloud reflection increases as ice crystal sizes become smaller, but the cloud absorption increase is only evident for wavelengths longer than about 2.7 μm. The ice crystal shape has a substantial effect on the cloud reflection and absorption for a given size; more complex ice particles reflect more solar radiation. Finally, we propose a contrail cirrus cloud model consisting of a combination of bullet rosettes (50%), hollow columns (30%), and plates (20%), with sizes ranging from 1 to 90 μm in association with radiation perturbation studies.

Introduction

One of the fundamental objectives of Subsonic Aircraft: Contrail and Cloud Effects Special Study (SUCCESS) is to provide the necessary and sufficient data to better determine the radiative properties of contrail cirrus and their potential impact on climate. Contrails tend to form in the vicinity of the tropopause in which the ambient temperature allows supersaturated water vapor emitted from jet engines to effectively convert into ice phase. Resident times for particles may vary from days below the tropopause and up to a year above the tropopause in the lower stratosphere. Analysis of air traffic patterns illustrates that, in general, cruising altitudes are within contrail cirrus producing levels. A number of statistical studies have indicated a significant correlation between jet fuel consumption and high cloud frequencies in urban airports [*Liou et al.*, 1990; *Frankel et al.*, 1997]. In particular, the data from Salt Lake City appear to support the connection between increasing jet aircraft operations in the upper troposphere, cirrus cloud cover, and regional climate when a sharp increase in domestic air traffic occurred in the mid-1960s.

Because of the lack of *in situ* microphysical observations in contrails, their radiative properties are largely unknown. The unique SUCCESS field experiment carried out over Kansas in April-May, 1996 provided microphysical measurements on the size and shape characteristics of ice crystals that were not available in the past. Using the observed ice crystal size distributions and shape factors for contrails, we have performed scattering and absorption calculations based on a unified theory for light scattering by ice crystals introduced in the text. Pertinent results for the extinction coefficient, single-scattering albedo, and phase function for contrail cirrus are presented. Employing a line-by-line equivalent solar model, we have also determined the spectral and broadband radiative properties of contrail cirrus.

Ice Crystal Size Distributions

During SUCCESS on May 4, 1996, ice crystal size distributions for the contrails were measured by the replicator system mounted on NASA's DC-8 that tailed a Boeing 757 by about 50 *sec* with aircraft separation distance of 11.5 *km* over northeast Oklahoma. This replicator system was developed by the scientists at the Desert Research Institute (DRI), University of Nevada [*Arnott et al.*, 1994]. Two representative ice crystal size distributions, associated with the ambient temperature and dew point of -61.1°C and -62.9°C, respectively, were selected for the present study. The growth of ice crystals in the contrails took about 50 *sec*. The ice crystal images collected by the DRI replicator system show that they were predominately bullet rosettes, columns, and plates with sizes ranging from about 1 μm to about 90 μm.

In addition to the preceding data, we have also obtained two ice crystal size distributions from an experiment sponsored by the Department of Energy that was carried out over the Cloud and Radiation Testbed (CART) site located in Northern Oklahoma and Southern Kansas on April 18 and 19, 1994. On 18 April, a contrail was studied above the CART site when the University of North Dakota Citation aircraft re-penetrated its own contrail after 6 *min* of growth at a height of 13 *km* and a temperature of -65.9°C. As shown in *Sassen* [1997], the DRI replicator indicated minute, simple plate and column crystals in the contrail. The data for 19 April, on the other hand, came from near the top (13.4 *km* and -69.4°C) of an optically thin cirrostratus cloud with embedded contrails, which contained minute solid ice particles. Since this cloud generated a lunar corona display, as contrails frequently do, we consider this cloud composition as a proxy of a persisting contrail. The size distribution data were derived from the FSSP device, which has been shown to yield reliable data when appreciable numbers of ice crystals larger than 50-100 μm are not present [*Gayet et al.*, 1996].

To characterize the effect of ice crystal size distributions on the radiative transfer results and to account for various shapes and sizes, we define the mean effective ice crystal size in terms of the maximum dimension, D, in the form

$$D_e = \int Vn(D)dD \Big/ \int An(D)dD = \frac{IWC/\rho_i}{A_t}, \quad (1)$$

where V and A are the volume and projection area of an ice crystal, respectively, IWC is the ice water content,

[1]Department of Atmospheric Sciences, University of California, Los Angeles, California.
[2]University of Utah, Salt Lake City, Utah.
[3]Langley Research Center/NASA, Hampton, Virginia.
[4]Desert Research Institute, Reno, Nevada.

Paper number 97GL03508.
0094-8534/98/97GL-03508$05.00

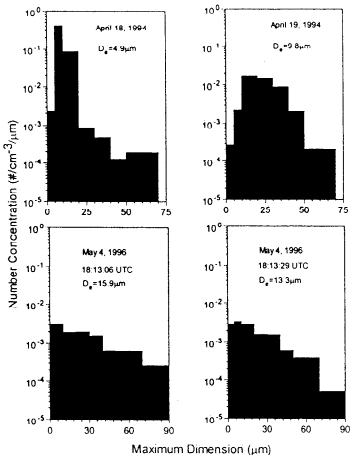

Figure 1. Discretized ice crystal size distributions for contrail cirrus (~ 50 sec duration) measured by the replicator system mounted on NASA's DC-8 that tailed a Boeing 757 during SUCCESS on May 4, 1996, and for a contrail and a cold cirrus (~ 6 min duration) measured by FSSP on board the University of North Dakota Citation on April 18 and 19, 1994 (upper panel).

ρ_i is the bulk ice density, and A_t is the projected area per unit volume. The mean effective ice crystal size so defined is now directly related to IWC, a prognostic parameter in GCMs. Also, by using the volume and projection area, the irregular ice crystal shape can be accounted for. Finally, A_t can be determined directly from the ice crystal images.

For single-scattering calculations, the observed ice crystal size distributions are discretized in eight bins: 1–5 μm with bin-center at 3 μm; 5–10 μm with bin-center at 7.5 μm; 10–20 μm with bin-center at 15 μm; 20–30 μm with bin-center at 25 μm; 30-40 μm with bin-center at 35 μm; 50–70 μm with bin-center at 60 μm; 70-90 μm with bin-center at 80 μm. Shown in Figure 1 are the discretized ice crystal size distributions. A substantial number of small ice crystals on the order of 10 μm is seen for the contrail that occurred on April 18, 1994.

Based on the SUCCESS replicator data, we estimate that contrails consist approximately of 50% bullet rosettes, 30% hollow columns, and 20% plates. Using these combinations, the mean effective sizes for the four ice crystal size distributions are 4.9, 9.8, 15.9, and 13.3 μm. The contrails observed on April 18 and 19 contain smaller ice particles than those observed on May 4.

Phase Function and Single-Scattering Properties

We have used the Monte-Carlo/geometric-ray-tracing approach to determine the scattering, absorption, and polarization properties of plates, solid and hollow columns, dendrites, bullet rosettes, aggregates, and ice crystals with irregular surfaces whose sizes are much larger than the incident wavelength [*Takano and Liou,* 1995]. For light scattering by small ice crystals, we have innovated an improved geometric-ray-tracing method and a finite-difference time domain (FDTD) method [*Yang and Liou,* 1996a,b]. The improved model is applicable to size parameters as small as about 15. The FDTD method is a numerical technique for the solution of the Maxwell equations in time and space using appropriate absorbing boundary conditions. It is considered to be

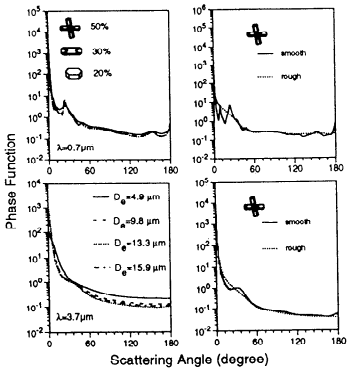

Figure 2. Phase functions for 0.7 and 3.7 μm wavelengths using a contrail cirrus model consisting of 50% bullet rosettes, 30% hollow columns, and 20% plates (left panel). The effect of ice crystal surface roughness on phase function is shown in the right panel using bullet rosette as an example.

the exact numerical solution for light scattering by particles, as verified by the exact theoretical solutions for long circular cylinders and spheres. Because of numerical round-off errors and required computer CPU time, the FDTD method can only be applied to ice crystal size parameters smaller than about 10-15. By unifying the modified geometric optics and FDTD methods for large and small size parameters, respectively, we are now in a position to determine the basic scattering, absorption, and polarization properties of ice crystals of any sizes and shapes that can be defined numerically.

The single-scattering parameters in terms of phase function, single-scattering albedo, and extinction cross section are computed for the solar spectrum covering 0.2 to 5 μm for about 200 wavelengths. The diagrams in the left panel in Figure 2 show the phase functions for the wavelengths of 0.7 and 3.7 μm. Substantial differences in the phase function for the four cases are noted at 3.7 μm at which ice is strongly absorptive and the ice crystal size has a significant impact on the single-scattering feature. For the case of 4/18/94, the halo peaks and backscattering for the 0.7 μm reduce substantially because of small ice crystal sizes.

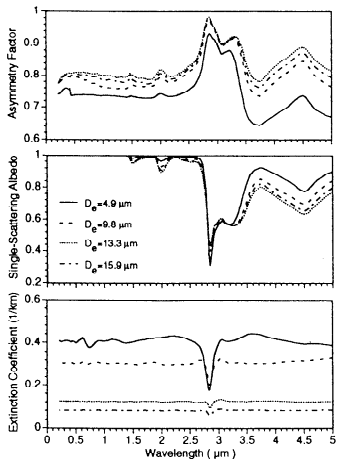

Figure 3. Asymmetry factor, single-scattering albedo, and extinction coefficient as functions of wavelength from 0.2 to 5 μm. The minima located at 2.85 μm are the well-known Christiansen effect.

From the replicator data, it appears that some ice crystals may not be exactly hexagonal in shape and that some may have rough surfaces. Following *Takano and Liou* [1995], we have used a Monte-Carlo/geometric-ray-tracing approach to account for the Fresnelian interactions between rays and rough surfaces of an ice crystal defined by the first-order Gram Charlier Series distribution [*Cox and Munk*, 1954]. The diagrams in the right panel of Fig. 2 illustrate the phase function differences between smooth and rough surfaces using bullet rosettes as an example. The smooth-surface bullet rosettes produce halo peaks at 22°, 46°, and 10°, as well as the backscattering peak and a maximum feature at about 150° at 0.7 μm. All of these peak features are smoothed out when the roughness on the surface is incorporated in the light scattering calculations. For strongly absorptive cases, the effect of surface roughness on the phase function for randomly oriented ice crystals is small because the scattering features are generated primarily by external reflections.

Figure 3 shows the asymmetry factor, single-scattering albedo, and extinction coefficient based on the shape model of 50% bullet rosettes, 30% hollow columns, and 20% plates. The extinction coefficients show little variation, except for a minimum in the 2.85 μm region, the so-called Christiansen effect. This effect occurs when the real part of the refractive index approaches 1 while the corresponding imaginary part is substantially larger, leading to the domination of absorption in light attenuation. It is particularly pronounced when ice particles are small, such as the 4/18/94 case. The single-scattering albedo also displays a strong minimum in the 2.85 μm region with values much less than 0.5. When absorption is substantial, the scattered energy is primarily contributed by diffraction in the forward directions. For this reason, maximum values of the asymmetry factor are noted around 3 μm. Introducing the roughness of ice crystal surfaces does not significantly affect the extinction coefficient and single-scattering albedo patterns. It should also be noted that soot particles can be activated as ice nuclei in contrail formation and the effect on the scattering and absorption of ice particles is dependent on their relative sizes.

Spectral and Broadband Solar Albedos

We have developed a new solar radiation model with a high spectral resolution similar to line-by-line calculations in the thermal IR, hereafter referred to as the line-by-line equivalent (LBLE) solar model. The spectral resolution has two options: 1 cm^{-1} with 10 g's and 50 cm^{-1} with 30 g's, where g denotes the cumulative probability function in the correlated k-distribution method. The correlated k-coefficients for these spectral intervals for H_2O from 2,000 to 21,000 cm^{-1} (0.5–5 μm) are determined from the updated 1996 HITRAN data based on the method developed by *Fu and Liou* [1993]. The correlated k-coefficients for the 2.0 and 2.7 μm CO_2 bands are also derived, in which overlaps between H_2O and CO_2 lines are accounted for by means of the multiplication rule. Absorption due to O_3 and O_2 bands and Rayleigh scattering contributions are accounted for based on the conventional method. In addition to cloud particles, we have also compiled the single-scattering properties of six typical aerosol in connection with the LBLE solar model.

The "exact" adding/doubling radiative transfer program including full Stokes parameters developed by *Takano and Liou* [1989] is used to calculate the transfer of monochromatic solar radiation in a vertically inhomogeneous atmosphere which is divided into 51 layers. For wavelengths between 3.7 to 5 μm, thermal emission

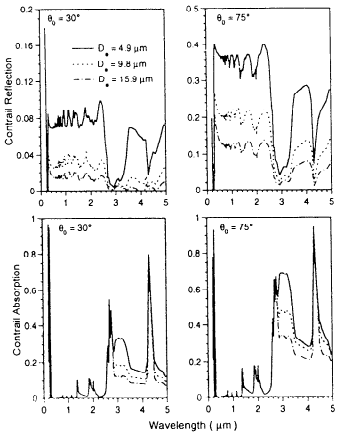

Figure 4. Spectral reflection and absorption for contrail cirrus as a function of the mean effective ice crystal size for two solar zenith angles. The contrail cirrus were located at 12 km over a land surface with a Lambertian albedo of 0.2 and with an IWP of 1 gm^{-3}.

contributions to the solar flux transfer are accounted for by adding the thermal emission part, $(1-\tilde{\omega})\pi B_\lambda(T)$, to the adding/doubling method, where $\tilde{\omega}$ is the single-scattering albedo and $\pi B_\lambda(T)$ is the Planck flux for a given temperature. The thermal part, although small, has not been accounted for in broadband solar flux calculations and could be a noticeable energy source in the upper part of the atmosphere; a subject for future exploration. The spectral solar radiative transfer program also includes the options of using the detailed solar irradiance data averaged over appropriate spectral resolutions.

Figure 4 illustrates the spectral reflection and absorption for the contrail layer as a function of the mean effective ice crystal size for two solar zenith angles of 30° and 75°. To economize the computations, we have used the spectral version of 50 cm^{-1} containing 30 g's. From observations, the contrails were located at about 12 km over a land surface which is assumed to have a Lambertian albedo of 0.2. In the calculations, we have employed an ice water path (IWP) of 1 gm^{-2}. The visible optical depth for an ice crystal cloud can be expressed in terms of both IWP and ice crystal size in the form [*Fu and Liou*, 1993]

$$\tau_v = IWP(a + b/D_e), \tag{2}$$

where a and b are certain coefficients. Thus, for a given IWP, the cloud reflection is inversely proportional to the mean effective ice crystal size D_e, as illustrated in Fig. 4. The water vapor absorption bands located at 3.2, 2.7, 1.87, 1.38, 1.1, 0.94, 0.82, and 0.72 μm are clearly shown, as is the 4.3 μm carbon dioxide band. The large reflection in the UV region is primarily produced by Rayleigh scattering. For the solar zenith angle of 75°, substantial reflection is evident for wavelengths shorter than about 2.5 μm, particularly for smaller D_e. The effect of ice crystal size on cloud absorption appears only for wavelengths greater than 2.8 μm, at which absorption due to ice particles becomes more significant than absorption due to water vapor and carbon dioxide.

The broadband reflection and absorption for contrail layers as a function of IWP are shown in Figure 5. The left and right panels illustrate the effects of ice crystal size and shape on the cloud radiative properties, respectively. In the calculations, we have used a solar zenith angle of 30° and a surface albedo of 0.2. Other input

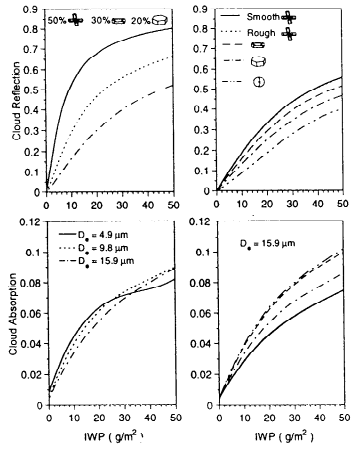

Figure 5. Broadband reflection and absorption for contrail cirrus as a function of IWP to illustrate the effects of ice crystal size (left panel) and shape (right panel). The solar zenith angle used is 30°.

parameters are the same. Cloud reflection for a given IWP is clearly dependent on ice crystal size: smaller ice crystals reflect more solar radiation than larger ice crystals. When IWP is smaller than about 20 gm^{-2}, cloud absorption also reduces when the ice crystal size increases. For IWP larger than about 20 gm^{-2}, cloud absorption for the case of 4.9 μm becomes the smallest because it is now determined by the single-scattering albedo rather than the optical depth. To investigate the shape effect, we have used a D_e of 15.9 μm. The effect of roughness of bullet rosette surfaces on cloud reflection and absorption is insignificant. Cloud reflection values become progressively smaller for hollow columns, plates, and equal-area spheres because their asymmetry factors become increasingly larger to allow stronger forward scattering to occur. Cloud absorption values for plates, hollow columns, and equal-area spheres become larger because of the progressively smaller single-scattering albedo values.

Summary

We have analyzed two ice crystal size distributions for contrail cirrus collected during SUCCESS and obtained two additional distributions from an experiment that was carried out earlier over the DOE CART site. Using these four observed ice crystal size distributions, we have performed the scattering and absorption calculations to determine the single-scattering and phase function properties of ice particles that were present in contrails for wavelengths from 0.2 to 5 μm. Based on the SUCCESS *in situ* observed data, we propose an ice crystal shape model for contrails consisting of 50% bullet rosettes, 30% hollow columns, and 20% plates in conjunction with radiation calculations.

For strongly absorptive cases, the ice crystal surface roughness is not a significant factor in determining the phase function pattern. The extinction coefficient shows a minimum feature at 2.85 μm referred to as the Christiansen effect, particularly pronounced when small ice crystals are present. The corresponding single-scattering albedo in this spectral region shows values much less than 0.5. Increasing the ice crystal size increases the asymmetry factor, whereas the reverse is true for the single-scattering albedo.

Based on a LBLE solar model, the dependence of cloud reflection on the mean effective ice crystal size for a given IWP is clearly illustrated in the entire solar spectrum. For a given IWP, smaller ice crystals reflect more solar radiation than larger ice crystals. The ice crystal shape has a substantial effect on the reflection and absorption calculations. For a given ice crystal size, cloud reflection values decrease progressively when bullet rosettes, hollow columns, plates, and equal-area spheres are employed in the calculations.

In order to investigate reliably the radiative and climatic effects of contrail cirrus, an appropriate ice crystal model in terms of size and shape is required. We have proposed a combination of bullet rosettes, hollow columns, and plates with sizes ranging from 1 to 90 μm for contrail cirrus in association with radiation perturbation studies. Finally, the subject of the finite and inhomogeneous nature of contrail cirrus on the radiative effects is one that requires further investigation.

Acknowledgments. This study was supported by NASA Grants NAG5-2678, NAG2-923, and NCC1- 189, AFOSR Grant F49620-94-1-0142, and by the Department of Energy Grants DE-FG03-95ER61991 and DE-FG03-94ER61747.

References

Arnott, W. P., Y. Y. Dong, and J. Hallett, Role of small ice crystals in radiative properties of cirrus: A case study, FIRE II, November 22, 1991, *J. Geophys. Res., 99,* 1371-1381, 1994.

Cox, C., and W. Munk, Measurement of the roughness of the sea surface from photographs of the sun's glitter, *J. Opt. Soc. Am., 44,* 838-850, 1954.

Frankel, D., K. N. Liou, S. C. Ou, D. P. Wylie, and P. Menzel, Observations of cirrus cloud extent and their impacts to climate, *Proceedings for the Ninth Conference on Atmospheric Radiation,* Am. Meteor. Soc., February 2-7, 1997, Long Beach, CA, 414-417, 1997.

Fu, Q., and K. N. Liou, Parameterization of the radiative properties of cirrus clouds, *J. Atmos. Sci., 50,* 2008-2025, 1993.

Gayet, J.-F., G. Febvre, and P. Larson, The reliability of the PMS FSSP in the presence of small ice crystals, *J. Atmos. Ocean. Tech., 13,* 100-1310, 1996.

Liou, K. N., S. C. Ou, and G. Koenig, An investigation on the climatic effect of contrail cirrus, in *Air Traffic and the Environment Background, Tendencies and Potential Global Atmospheric Effects,* edited by U. Schumann, pp. 154-169, Springer Verlag, 1990.

Sassen, K., Contrail-cirrus and their potential for regional climate change, *Bull. Amer. Meteor. Soc., 78,* 1885-1903, 1997.

Takano, Y., and K. N. Liou, Solar radiative transfer in cirrus clouds. II: Theory and computation of multiple scattering in an anisotropic medium, *J. Atmos. Sci., 46,* 20-36, 1989.

Takano, Y., and K. N. Liou, Radiative transfer in cirrus clouds. III: Light scattering by irregular ice crystals, *J. Atmos. Sci., 52,* 818-837, 1995.

Yang, P., and K. N. Liou, Finite-difference time domain method for light scattering by small ice crystals in three-dimensional space, *J. Opt. Soc. Am. A., 13,* 2072-2085, 1996a.

Yang, P., and K. N. Liou, Geometric-optics-integral-equation method for light scattering by nonspherical ice crystals, *Appl. Opt., 35,* 6568-6584, 1996b.

K. N. Liou, P. Yang, and Y. Takano, Department of Atmospheric Sciences, UCLA, Los Angeles,CA 90095-1565

K. Sassen, Department of Meteorology, University of Utah, Salt Lake City, UT 84112

T. P. Charlock, Atmospheric Sciences Division, Langley Research Center/NASA, Hampton, VA 23665

W. P. Arnott, Atmospheric Sciences Center, Desert Research Institute, Reno, NV 89506

(Received July 10, 1997; revised November 20, 1997; accepted November 25, 1997.)